$Os(H)_2NO(P^iPr_3)_2^+$: Mechanism and Energetics of a Room Temperature Reversible Ethyl/Hydridoethylene Equilibrium and Contrasting Double Insertion of Acetylene

Dmitry V. Yandulov, John C. Bollinger, William E. Streib, and Kenneth G. Caulton*

Department of Chemistry, Indiana University, Bloomington, Indiana 47405-7102

Received October 23, 2000

cis,trans-$Os(H)_2(NO)L_2^+$ (L = P^iPr_3) rapidly adds ethylene to give an η^2-ethylene complex with C_2H_4 trans to one hydride and cis to the other. *One* hydride and the four ethylene protons are exchanging reversibly above −20 °C, with a measured $\Delta G^‡$ (20 °C) of 15 kcal/mol. DFT calculations on the rearrangement reveal bond making and breaking, as well as migration of the nonexchanging hydride. Nitrosyl bending is not involved. Use of acetylene leads to insertion into both Os−H bonds; the resulting $Os(CH{=}CH_2)_2(NO)L_2^+$ was fully characterized as having inequivalent vinyl groups and undergoes facile vinyl ligand site exchange in solution.

Introduction

We reported earlier[1] that $NaBAr'_4$ (Ar′ = 3,5-$(CF_3)_2$-C_6H_3) abstracts chloride from $Os(H)_2Cl(NO)L_2$ (L = P^iPr_3, **1-Cl**) to form a highly Lewis acidic cation **1-$CH_2Cl_2^+$** (BAr'_4). The equilibrium (1) does not lie fully

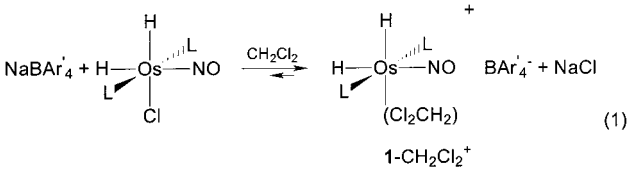

(1)

to the right at a 1:1 stoichiometry, even with the thermodynamic assistance given by coordination of CH_2Cl_2 to the cation. Only in toluene/C_6H_5F mixed solvent can one form the authentic unsaturated, five-coordinate cation $\mathbf{1}^+$, and it has a square-pyramidal structure with

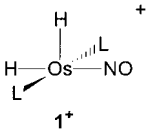

inequivalent hydrides; these show exceptionally different chemical shifts (−19.4 and +4.0 at −55 °C), when their site-exchange fluxionality is decoalesced.

The equilibrium system in eq 1 is quite reactive under mild conditions, and we report here its reaction with the potentially reducible substrates C_2H_4 and C_2H_2.

Results

Ethylene Adduct of $[Os(H)_2(NO)L_2]^+$. Exposure of an equilibrium mixture of **1-Cl** and **1-$CH_2Cl_2^+$**, generated from **1-Cl** and 1.05 equiv of $NaBAr'_4$ in CH_2Cl_2, to an atmosphere of ethylene resulted in a rapid color change from yellow-orange to pale lemon-yellow; NMR spectra showed quantitative formation of a single product. Equilibrium 1 with X = Cl is shifted completely to the right, as the unsaturated $\mathbf{1}^+$ is stabilized by coordination of an ethylene molecule. The product, isolated in 92% yield, was characterized as [*cis,trans*-$Os(H)_2(\eta^2\text{-}C_2H_4)(NO)(P^iPr_3)_2$][$BAr'_4$] (**1-$C_2H_4^+$**). The solid-state structure of **1-$C_2H_4^+$(BAr'_4)** was found to be plagued by extensive disorder, but the otherwise identical PF_6^- salt could be prepared analogously with $AgPF_6$, albeit in lower yield, and allowed an X-ray structure determination (Figure 1, Table 1). The cation **1-$C_2H_4^+$** adopts a strongly distorted octahedral geometry, in which the ethylene unit is aligned perpendicular to the H(2)−Os−N plane in an orientation highly unfavorable sterically, due to the repulsion with the bulky P^iPr_3 ligands. The latter two bend away from η^2-C_2H_4, toward H(2), to an unusually small P(5)−Os−P(5a) angle of 145° (Table 2), which is apparently responsible for the lack of virtual coupling to the (PC)Me groups in ^1H NMR. This type of distortion has been previously found for the isoelectronic $OsH(OH)(CO)(\eta^2\text{-}CH_2{=}CHCO_2CH_3)(P^iPr_3)_2$,[2] in which an even bulkier olefin also adopts an orientation with C=C approximately collinear with the P−Os vectors, leading to the small P−Os−P angle of 144°.

The orientation of ethylene in **1-$C_2H_4^+$** is determined electronically, so as to allow for efficient back-bonding from a filled Os d_π orbital that is not involved in the back-bonding to NO. However, the bending of the phosphines, which alleviates the repulsion with the olefin, also forces rehybridization of the filled Os d_π orbital involved in the bonding with ethylene, as shown in Scheme 1. This three-orbital/four-electron interaction

* To whom correspondence should be addressed. e-mail: caulton@indiana.edu.

(1) Yandulov, D. V.; Streib, W. E.; Caulton, K. G. *Inorg. Chim. Acta* **1998**, *280*, 125.

(2) Edwards, A. J.; Elipe, S.; Esteruelas, M. A.; Lahoz, F. J.; Oro, L. A.; Valero, C. *Organometallics* **1997**, *16*, 3828.

10.1021/om000901g CCC: $20.00
Publication on Web 03/29/2001

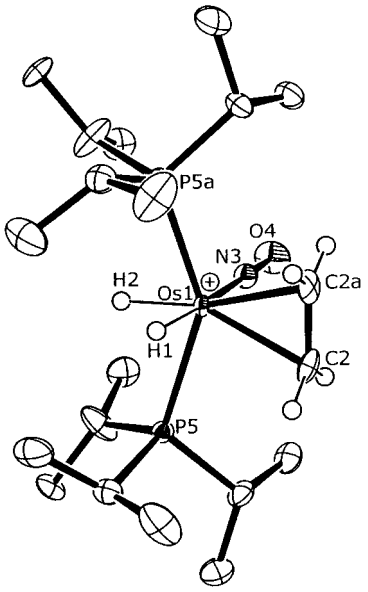

Figure 1. ORTEP representation of the cation of [cis,-trans-$Os(H)_2(C_2H_4)(NO)(P^iPr_3)_2$][$PF_6$]. The structure has a crystallographic plane of symmetry, passing through H2, Os1, N3. Ellipsoids are drawn to 50% probability level. Phosphine hydrogens were omitted for clarity.

Table 1. Crystallographic Data for 1-$C_2H_4^+$ (PF_6^-) and 4

	1-$C_2H_4^+$ (PF_6^-)	4
formula	$C_{20}H_{49}F_6NOOsP_3$	$C_{54}H_{60}BF_{24}NOOsP_2$
space group	*Pnma*	*C2/c*
T, °C	−160	−160
a, Å	14.396(2)	17.0982(7)
b, Å	22.926(2)	18.3641(7)
c, Å	8.603(1)	19.8362(7)
α, Å		107.3480(10)
ρ_{calcd}, g/cm^{-3}	1.674	1.629
μ(Mo Kα), cm^{-1}	47.1	23.12
V, Å^3	2839.28	5945.12
Z	4	4
formula weight	715.75	1458.03
R	0.0380	0.058
R_w	0.0362	0.149

[a] $R = \sum||F_o| - |F_c|\sum|F_o|$. [b] $R_w = [\sum w(|F_o| - |F_c|)^2/\sum w|F_o|^2]^{1/2}$ where $w = 1/\sigma^2(|F_o|)$.

Table 2. Selected Bond Lengths (Å) and Angles (deg) in $Os(H)_2(C_2H_4)(NO)(P^iPr_3)_2^+$

Os(1)−P(5)	2.4161(18)
Os(1)−N(3)	1.779(8)
Os(1)−C(2)	2.247(6)
N(3)−O(4)	1.178(10)
Os(1)−H(1)	1.48
Os(1)−H(2)	1.44
C(2)−C(2a)	1.418(15)
P(5)−Os(1)−P(5a)	145.14(8)
C(2)−Os(1)−C(2a)	36.8(4)
H(1)−Os(1)−H(2)	71.3
Os(1)−N(3)−O(4)	179.5(8)
P(5)−Os(1)−N(3)	99.28(8)
N(3)−Os(1)−H(1)	174.8
N(3)−Os(1)−H(2)	103.4

is fully analogous to the "push−pull" interactions[3] with the π-symmetry combination of the P σ-bonding orbitals acting in place of a filled π-orbital. In the case of 1-$C_2H_4^+$, it stabilizes the sterically unfavorable geometry by increasing the back-bonding to the olefin, but

(3) Caulton, K. G. *New J. Chem.* **1994**, *18*, 25.

Scheme 1

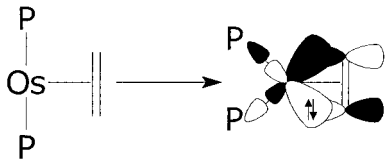

the repulsion between the phosphines limits the extent of the structural distortion.

The solid-state structure of 1-$C_2H_4^+$ shows that ethylene adopts an orientation that is not suitable for insertion into the *cis*-Os−H bond. However, solution ^{1}H NMR spectra show operation of this insertion as a facile intramolecular fluxionality (Figure 2). Thus, the ordinary AMX_2 pattern in the hydride region ($X = ^{31}P$, J(A−M) = 8.0 Hz), observed in the limit of stopped exchange, is devoid of A−M coupling at 20 °C, and additionally, one hydride and the ethylene signals (coalesced, intensity 4) are considerably broadened. Closer examination of the low-field hydride resonance (Figure 2) shows that the J(P−H) triplet (−3.34 ppm) is additionally split into a sextet ($J \approx 1.9$ Hz), which quite unambiguously demonstrates that (a) the exchange is intramolecular and (b) a single hydride ligand is involved in the site-exchange with all four ethylene protons. Measurement of the increase in the line width of the C_2H_4 signal gives an estimate of the exchange barrier as $\Delta G^{\ddagger} = 15$ kcal/mol at 20 °C. Reversible insertion of the olefin into the *cis*-Os−H bond, followed by exchange of agostic β-hydrogens of the ethyl ligand and β-hydride elimination, appears as a reasonable mechanism for the observed fluxionality.

Computational Study of the H/C_2H_4-to-Ethyl Equilibrium. DFT calculations (B3LYP/LANL2DZ) (Figure 3) on the simplified model [$Os(H)_2(C_2H_4)(NO)(PH_3)_2$]$^+$ largely support the proposed mechanism. Thus, facile 90° rotation of the ethylene ligand leads to a minimum with an orientation suitable for insertion, and insertion occurs as the rate-determining step to give a β-hydride agostic *trans*-hydrido ethyl structure (**A**). The latter easily rearranges by simultaneous loss of the agostic interaction and migration of the hydride to the site trans to NO to give a relatively stable square-pyramidal minimum with apical ethyl, devoid of agostic stabilization of the metal. Rotation of the methyl group couples with the latter rearrangement at later stages and completes the exchange of a hydrogen originating from Os and one from C_2H_4. The computed activation energy of 11.6 kcal/mol (9.7 with ZPE) is rather low, as compared to the experimental estimate, likely due to the underestimation of the phosphine donor power and neglect of ion-pairing and electrostatic interactions present in solution with the experimental 1-$C_2H_4^+$ cation. The poor reducing ability of the metal center in 1-$C_2H_4^+$ is in fact directly responsible for the observed facile insertion of the olefin, as the isoelectronic neutral carbonyl analogues $Os(H)_2(\eta^2\text{-}H_2C{=}CHR)(CO)(P^iPr_3)_2$ (R = Et,[4a] Ph[4b]) fail to reveal analogous fluxional

(4) (a) Albéniz, M, J.; Buil, M. L.; Esteruelas, M. A.; López, A. M. *J. Organomet. Chem.* **1997**, *545*−*546*, 495. (b) Espuelas, J.; Esteruelas, M. A.; Lahoz, F. J.; Oro, L. A.; Valero, C. *Organometallics* **1993**, *12*, 663.

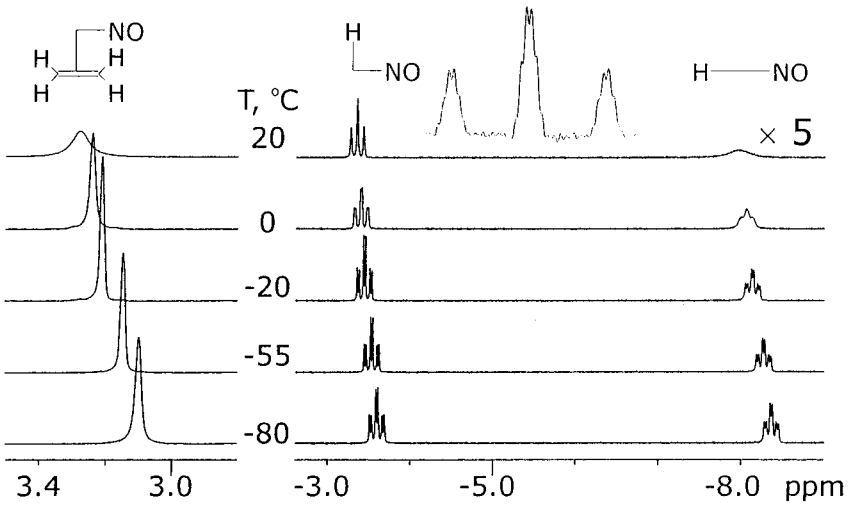

Figure 2. Variable temperature 300 MHz ^{1}H NMR spectra of **1-C_2H_4**$^+$ (BAr'_4) in CD_2Cl_2 with signal assignments, showing the effects of reversible insertion of ethylene into cis-Os−H bond. The inset on top shows additional sextet coupling in the signal of the hydride *cis* to NO (resolution−enhanced) at +20 °C.

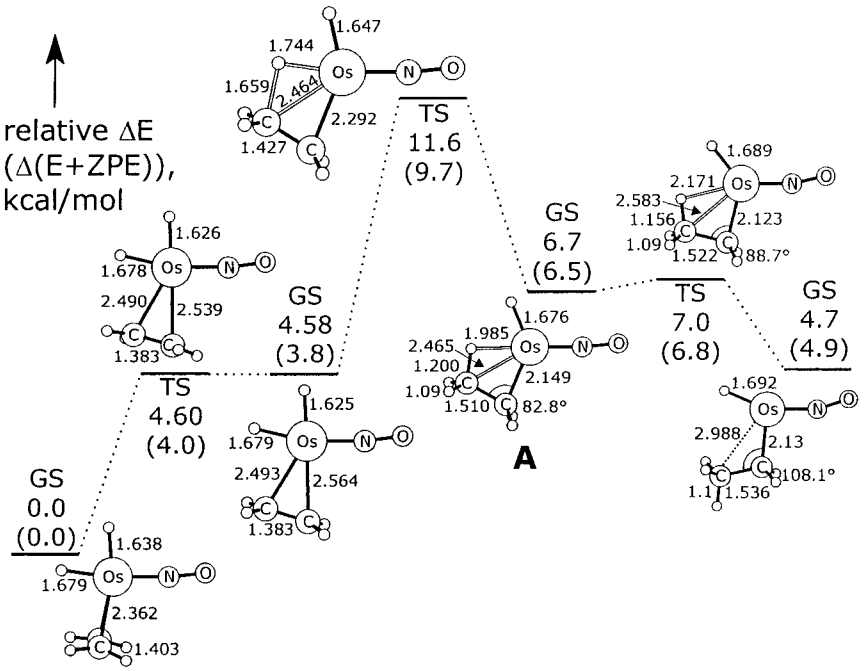

Figure 3. Structures involved in the intramolecular (Os)H ↔ (C)H exchange in $Os(H)_2(C_2H_4)(NO)(PH_3)_2^+$, relative energies and selected geometric parameters (Å, °). trans-PH_3 groups were omitted for clarity.

processes under ambient conditions. Notably, similarly static is the neutral derivative $OsH(\eta^2\text{-}C_2H_4)(NO)(P^iPr_3)_2$.[5]

Reactivity of $Os(H)_2(C_2H_4)(NO)L_2^+$ with Ethylene. The complex **1-C_2H_4**$^+$ decomposes under argon at room temperature on the time scale of days in d_8-PhMe/PhF or CD_2Cl_2 solution into several uncharacterized products; evolution of ethane was detected by ^{1}H NMR in CD_2Cl_2 solvent. Under an atmosphere of ethylene, however, a fairly clean transformation takes place, generating the methallyl $OsH(\eta^3\text{-}H_2CCHCHMe)(NO)(P^iPr_3)_2^+$ (**2**) as the predominant product. The identity of **2** was established by NMR and its independent synthesis from **1-Cl**, $NaBAr'_4$, and butadiene. Heating a d_8-PhMe/PhF solution of **1-C_2H_4**$^+$ under 1 atm of C_2H_4 at 58 °C gave 75% conversion into **2** after 2 h and nearly 100% after 16 h. The ^{1}H NMR spectrum of the volatiles from this reaction mixture revealed the presence of ethane, 1-butene, *cis*- and *trans*-2-butene and butadiene, all in comparable amounts. This result shows that although **1-C_2H_4**$^+$ is active for ethylene dimerization, the presence of a second hydride leads to catalyst deactivation, i.e., formation of **2**, by hydrogenation of ethylene and subsequent ethylene C−H oxidative addition, as a plausible mechanism.

Reactivity of $Os(H)_2(C_2H_4)(NO)L_2^+$ with Cl^-. Reaction of **1-C_2H_4**$^+$ with Bu_4NCl (i.e., "reactive trapping") gave some evidence for the ready accessibility of isomeric structures with ethylene inserted into one of the Os−H bonds, as suggested by DFT calculations (Figure 3). Thus, dissolution of a solid mixture of **1-C_2H_4**$^+$ and Bu_4NCl in CD_2Cl_2 gave (eq 2), within 10 min, a mixture of $OsCl(NO)(P^iPr_3)_2$[6] (20%), $Os(H)_2Cl(NO)L_2$ (4%), and

(5) Yandulov, D. V.; Caulton, K. G., in preparation.

a product assigned as OsHCl(Et)(NO)(P^{i}Pr$_3$)$_2$ (**3**) with H trans to Et and mutually *trans*-P^{i}Pr$_3$ (76%) on the basis of NMR data. Specifically, ^{1}H NMR revealed a

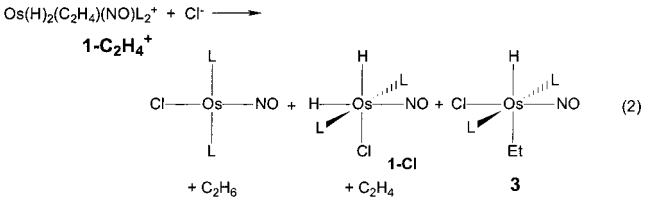

hydride triplet at −1.12 ppm (J_{P-H} = 24.3 Hz), integrating to 1 hydride against the PC*H* signal, diastereotopically shifted and virtually coupled PCC*H*$_3$ resonances, and a signal at 2.65 ppm, which simplified into a 7.8 Hz quartet on selective ^{31}P decoupling, assigned to CH$_2$ of the ethyl ligand, together with the 7.8 Hz triplet at 1.11 ppm (OsCH$_2$C*H*$_3$). The formation of Os(H)$_2$Cl(NO)L$_2$ is a result of simple ethylene displacement (detected by ^{1}H NMR); while trapping of a five-coordinate hydrido ethyl isomer with basal NO, followed by ethane reductive elimination (detected by ^{1}H NMR), can account for the formation of OsCl(NO)(P^{i}Pr$_3$)$_2$, **3** is a likely product of trapping of the inserted isomer **A** (Figure 3), in which the vacant coordination site trans to NO is occupied by a C−H agostic interaction. Notably, using d_8-PhMe/PhF as a solvent in the analogous reaction gave the same products in significantly different ratios, i.e., OsCl(NO)(P^{i}Pr$_3$)$_2$ (53%), Os(H)$_2$Cl(NO)L$_2$ (21%), and **3** (26%). Subjecting this reaction mixture to a 55 °C thermolysis for 22 h under Ar did not significantly alter its composition, consistent with the structure tentatively assigned to **3**, in which ethane reductive elimination is inhibited by the trans-disposition of H and Et and the structural rigidity of d^6 octahedral complexes. The synthesis of **1-C$_2$H$_4^+$** from **1-Cl** and C$_2$H$_4$ by Cl$^-$ abstraction and subsequent reactivity of **1-C$_2$H$_4^+$** by Cl$^-$ addition can be coupled in a dehydrogenation reaction of **1-Cl** with ethylene even *without* electrophiles assisting the Cl$^-$ loss: heating a THF solution of **1-Cl** under 1 atm of C$_2$H$_4$ at 90 °C for 19 h results in a 70% conversion of **1-Cl** into OsCl(NO)(P^{i}Pr$_3$)$_2$ as the major (90%) product. In contrast to the Cl$^-$ reaction, giving predominantly the trapping products of the inserted hydrido ethyl isomers of **1-C$_2$H$_4^+$**, Bu$_4$NOTf reacted in CD$_2$Cl$_2$ mainly by ethylene displacement, giving the osmium triflate Os(H)$_2$(OTf)(NO)(P^{i}Pr$_3$)$_2$[1] nearly quantitatively after several days at room temperature.

Reactivity of Os(H)$_2$(NO)L$_2^+$ with Acetylene. Subjecting the equilibrium mixture of **1-Cl** and **1-CH$_2$Cl$_2^+$** to an atmosphere of acetylene in CD$_2$Cl$_2$ resulted in a prompt development of a deep purple color and formation of a single product [Os(CH=CH$_2$)$_2$(NO)(P^{i}Pr$_3$)$_2$][BAr′$_4$] (**4**), isolated in 84% yield and fully characterized by NMR and X-ray diffraction. Under ambient conditions, several broad features are seen in the olefinic region by ^{1}H NMR, while the PCC*H*$_3$ signals do not reveal diastereotopic inequivalence. Cooling a CD$_2$Cl$_2$ solution of **4** results in gradual sharpening of the olefinic resonances; by −40 °C, ^{1}H NMR shows two well-resolved sets of vinyl signals, and the P^{i}Pr$_3$ methyl groups are now diastereotopically shifted, as expected for a square-pyramidal structure with an apical vinyl. This geometry was established by X-ray diffraction (Figure 4), which also revealed no unusual intramolecular contacts to the 16-e osmium, such as agostic interactions with the P^{i}Pr$_3$ C−H bonds or η^2-binding of a vinyl ligand, despite the notable observation of large and similar J_{HH} coupling constants (15 and 18 Hz) across the double bond at one vinyl ligand in the low temperature ^{1}H NMR. The structure was disordered around a center of symmetry. The unsaturated complex **4**, crystallized out of the CH$_2$Cl$_2$ reaction mixture containing excess acetylene, contains neither of these two potential ligands, which speaks for some steric crowding around the unsaturated metal. The fluxional solution behavior of **4** is therefore a result of facile vinyl ligand site-exchange, analogous to that found in the dihydride[1] analogue and common to other five-coordinate bis-phosphine square-pyramidal complexes with three strong trans-influence ligands in the symmetry plane.[7] Although it is possible that coordination of CD$_2$Cl$_2$ in solution at low temperatures locks the ligand site-exchange, as in the case of the cationic dihydride,[1] the absence of such an interaction in the solid state makes this stabilization unlikely. Coordination of a better ligand, such as Cl$^-$, does, however, stop the fluxional process, as treatment of **4** with Bu$_4$NCl in CD$_2$Cl$_2$ leads to appearance of two well-resolved vinyl features in ^{1}H NMR, assigned to the neutral *cis,trans*-Os(CH=CH$_2$)$_2$Cl(NO)(P^{i}Pr$_3$)$_2$.

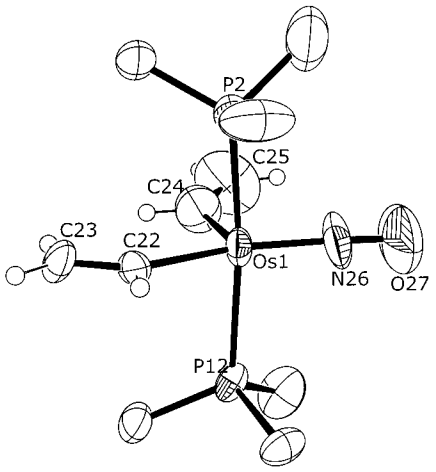

Figure 4. ORTEP representation of the cation Os(C$_2$H$_3$)$_2$(NO)(P^{i}Pr$_3$)$_2^+$. Methyls and all ^{i}Pr hydrogens have been omitted.

Table 3. Selected Bond Lengths (Å) and Angles (deg) for [Os(CHCH$_2$)$_2$(NO)(P^{i}Pr$_3$)$_2$]$^+$

Os(1)	N(26)	1.743(10)		Os(1)	P(2)	2.460(4)	
Os(1)	C(24)	1.994(13)		C(22)	C(23)	1.35(2)	
Os(1)	C(22)	2.063(10)		C(24)	C(25)	1.319(19)	
Os(1)	P(12)	2.440(4)		N(26)	O(27)	1.11(3)	
N(26)	Os(1)	C(24)	102.9(8)	C(24)	Os(1)	P(2)	91.9(4)
N(26)	Os(1)	C(22)	158.0(6)	C(22)	Os(1)	P(2)	83.9(4)
C(24)	Os(1)	C(22)	99.0(6)	P(12)	Os(1)	P(2)	166.24(14)
N(26)	Os(1)	P(12)	94.8(4)	C(23)	C(22)	Os(1)	135.7(13)
C(24)	Os(1)	P(12)	97.2(4)	C(25)	C(24)	Os(1)	134.3(13)
C(22)	Os(1)	P(12)	84.5(3)	O(27)	N(26)	Os(1)	175(2)
N(26)	Os(1)	P(2)	93.1(3)				

(6) Werner, H.; Flügel, R.; Windmüller, B.; Michenfelder, A.; Wolf, J. *Organometallics* **1995**, *14*, 612.

(7) Heyn, R. H.; Macgregor, S. A.; Nadasdi, T. T.; Ogasawara, M.; Eisenstein, O.; Caulton, K. G. *Inorg. Chim. Acta* **1997**, *259*, 5.

Conclusions

The special value of the computational study (Figure 3) is to put bond lengths and angles to both intermediates and transition states in the surprisingly fluxional dihydride ethylene cation. Key points are as follows:

(1) The energy of the nonagostic inserted species is as low as the energy of simply rotating η^2-C_2H_4 (~4 kcal/mol), despite the insertion being an 18-to-16-electron conversion. This is perhaps due to destabilization of the dihydride ethylene species: ethylene trans to the hydride has long Os−C distances[8] and thus diminished back-donation.

(2) There is no major bending of ∠Os−N−O throughout the rearrangements.

(3) The nonagostic ethyl species has a (square-pyramidal) coordination geometry analogous to that of $Os(H)_2(NO)L_2^+$.

(4) The loss of the agostic interaction during the *exothermic* conversion from the agostic ethyl **A** to the nonagostic ethyl is in fact *concerted* with hydride migration.

(5) The agostic ethyl is ~2 kcal/mol less stable than the nonagostic ethyl, apparently because the (weak) C−H donation (trans to NO) is offset by the cost of compressing ∠Os−C_α−C_β (to 82.8°) and the relocation of the hydride ligand.

It is also noteworthy that a reagent like $Os(H)_2(NO)L_2^+$, carrying two H ligands, easily makes an ethyl, but does not readily liberate ethane. This is apparently associated with the high energy for producing 14-valence electron zerovalent $Os(NO)L_2^+$.

The ready energetic accessibility of the hydride ethyl species from the dihydride ethylene global minimum structure of **1-$C_2H_4^+$** is the consequence of the overall cationic charge and the presence of the very strong π-acid, linear NO, which together reduce the back-bonding to the ethylene and destabilize the η^2-C_2H_4 isomer. Comparison to the neutral carbonyl analogues,[4] which do not exhibit reversible olefin insertion fluxionality, shows that the steric repulsion between the olefin and the bulky P^iPr_3 phosphines alone does not sufficiently destabilize the dihydride olefin isomer relative to the inserted hydride ethyl species. Thus, isoelectronic substitution of NO^+ for CO at relatively soft, reducing Os(II) creates a metal center with sufficiently hard Lewis acidic character to significantly stabilize the ethyl isomer relative to its H(η^2-C_2H_4) form. This feature of the electronic structure also determines the low activation energy for the olefin insertion/β-hydride elimination processes at Os, a 5d metal center generally viewed as kinetically inert.

Ethylene and acetylene react quite differently with $Os(H)_2(NO)L_2^+$, the former only once, and with η^2-coordination but without "full" insertion to an ethyl and the latter twice and each time with insertion. We have traced the origin of this to the generally greater thermodynamic stability derived from hydrogenating C≡C to C=C than for hydrogenating C=C to C−C.[9] Thus, C≡C inserts preferentially and, when it does, it leaves the metal unsaturated and available to bind another alkyne.

Experimental Section

General. All manipulations were carried out using standard Schlenk and glovebox techniques under argon, with flame-dried glassware (including NMR tubes). Bulk solvents were dried by appropriate methods, distilled, freeze−pump−thaw degassed, and stored over corresponding molecular sieves in gastight solvent bulbs with Teflon closures. C_6D_6, d_8-PhMe, and CD_2Cl_2 were dried accordingly, vacuum-transferred, degassed, and stored in an argon-filled glovebox. Na[B(C_6H_3-3,5-$(CF_3)_2)_4$] (NaBAr′$_4$)[10] and *cis*,*trans*-$Os(H)_2Cl(NO)(P^iPr_3)_2$[1] were synthesized by published procedures. ^{1}H and ^{31}P spectra were recorded on a Varian Gemini 2000 (^{1}H: 300 MHz; ^{31}P: 122 MHz) or a Varian Inova 400 (^{1}H: 400 MHz; ^{31}P: 162 MHz) spectrometers and referenced to the residual protio solvent peaks (^{1}H) or external 85% H_3PO_4 (^{31}P). Chemical shifts are reported in ppm relative to Me_4Si (^{1}H) and 85% H_3PO_4 (^{31}P). NMR probe temperatures from ambient to −100 °C were calibrated with a methanol standard. Samples were allowed at least 10 min to equilibrate at each temperature, which was maintained to ±0.5°. Infrared spectra were recorded on a Nicolet 510P FT-IR spectrometer. Elemental analyses were performed on a Perkin-Elmer 2400 CHNS/O Elemental Analyzer at Indiana University.

[$Os(H)_2$(η^2-C_2H_4)(NO)(P^iPr_3)$_2$][B(C_6H_3-3,5-$(CF_3)_2)_4$] (1-$C_2H_4^+$). A heterogeneous mixture of $Os(H)_2Cl(NO)L_2$ (100 mg, 0.173 mmol) and NaBAr′$_4$ (161 mg, 0.182 mmol) in CH_2Cl_2 (5 mL) was freeze−pump−thaw degassed and pressurized with 1 atm of C_2H_4. After stirring the resulting lemon-yellow mixture for 30 min, the solution was filtered through Celite, the solid washed with 3 × 5 mL of CH_2Cl_2, and the combined extracts were concentrated to ca. 4 mL and layered with pentane (15 mL). After standing at −20 °C for several days, the pale-yellow crystals formed were washed with pentane, dried in vacuo, and stored at −20 °C under Ar. Yield 229 mg (0.160 mmol, 92%). ^{1}H NMR (CD_2Cl_2, 20 °C): δ 7.72 (br, 8H, *o*-$C_6H_3(CF_3)_2$), 7.56 (s, 4H, *p*-$C_6H_3(CF_3)_2$), 3.28 (br. s, 4H, OsC_2H_4), 2.67 (approximately octet, $J_{PH} = J_{HH} = 7.2$ Hz, 6H, $PCH(CH_3)_2$), 1.27 (dd, $J_{HH} = 6.9$ Hz, $J_{PH} = 15.6$ Hz, 18H, $PCH(CH_3)_2$), 1.25 (dd, $J_{HH} = 6.9$ Hz, $J_{PH} = 15.6$ Hz, 18H, $PCH(CH_3)_2$), −3.35 (t of sextets, $J_{PH} = 23.4$ Hz, J_{HH}(av.) = 1.9 Hz, 1H, Os*H*), −7.9 (br. s, 1H, Os*H*). ^{31}P{^{1}H} NMR (CD_2Cl_2, 20 °C): δ 28.9 (s), hydride-only coupled: d. IR (CH_2Cl_2): 1777 cm^{-1} (ν_{NO}). Anal. Found (Calcd, %) for $C_{52}H_{60}BF_{24}NOOsP_2$: C 43.50 (43.56), H 3.87 (4.22), N 1.03 (0.98). Selected ^{1}H NMR (CD_2Cl_2, −55 °C): δ 3.15 (s, 4H, OsC_2H_4), −3.53 (td, J_{PH} = 23.7 Hz, $J_{HH} = 8.0$ Hz, 1H, Os*H*), −8.27 (td, $J_{PH} = 21.9$ Hz, $J_{HH} = 8.0$ Hz, 1H, Os*H*). The PF_6^- salt was prepared analogously, using 1.05 equiv of $AgPF_6$ in PhF solvent in the dark, and isolated by layering the PhF filtrate with pentane and recrystallizing the solid formed from CH_2Cl_2/pentane; a mixture of pale-yellow (majority) and dark orange-brown crystals was obtained, containing ca. 70% of **1-$C_2H_4^+$** (PF_6^-) by NMR, with the cation resonances nearly identical to those described above for the BAr′$_4^-$ salt. The pale-yellow crystals were used for X-ray structure determination.

Generation of [OsH(η^3-$H_2CCHCHMe$)(NO)(P^iPr_3)$_2$][B(C_6H_3-3,5-$(CF_3)_2)_4$] (2). To a solid mixture of $Os(H)_2Cl(NO)L_2$ and 1.1 equiv of NaBAr′$_4$ in an NMR tube fitted with a Teflon stopcock was added CH_2Cl_2 (0.6 mL). The mixture was freeze−pump−thaw degassed three times and subjected to an atmosphere of 1,4-butadiene. Following the vigorous shaking and stirring of the reaction mixture for 20 min, the resulting heterogeneous light-yellow solution was redissolved in CD_2Cl_2 and analyzed by NMR to reveal the presence of the title

(8) Johnson, T. J.; Albinati, A.; Koetzle, T. F.; Ricci, J.; Eisenstein, O.; Huffman, J. C.; Caulton, K. G. *Inorg. Chem.* **1994**, *33*, 4966.

(9) See however Nicolaides, A.; Borden, W. T. *J. Am. Chem. Soc.* **1991**, *113*, 6750.

(10) Brookhart, M.; Grant, B.; Volpe, A. F., Jr. *Organometallics* **1992**, *11*, 3920.

compound as essentially the only observable product. ^{1}H NMR (CD_2Cl_2, 20 °C): δ 7.72 (br, 8H, *o*-$C_6H_3(CF_3)_2$), 7.56 (s, 4H, *p*-$C_6H_3(CF_3)_2$), 5.45 (m, 1H, C*H*), 5.00 (m, 1H, C*H*), 2.47 (m, 6H, PC*H*$(CH_3)_2$), 1.94 (d, J_{HH} = 6.0 Hz, 3H, CCH_3), 1.65 (m, 1H, C*H*), 1.32 (m, 36H, PCH(CH_3)$_2$), 1.10 (m, 1H, C*H*), −4.21 (approximately t, J_{PH} = 24.0 Hz, 1H, Os*H*). ^{31}P{^{1}H} NMR (CD_2Cl_2, 20 °C): AB, δA = 16.91, δB = 16.09, J_{AB} = 176.5 Hz.

Reaction of 1-$C_2H_4^+$ (BAr'_4) with Bu_4NCl. To a solid mixture of **1-$C_2H_4^+$** (BAr'_4) and 1.5 equiv of Bu_4NCl in an NMR tube fitted with a Teflon stopcock was added CD_2Cl_2 (0.6 mL) to give a light brownish solution quickly developing a greenish hue. The ^{1}H NMR spectrum recorded within 10 min showed complete conversion of **1-$C_2H_4^+$** into a mixture of $Os(H)_2Cl(NO)L_2$[1] (4%), $OsCl(NO)(P^iPr_3)_2$[6] (20%), and a product assigned as $OsHCl(Et)(NO)(P^iPr_3)_2$ (**3**, 76%). For **3**: ^{1}H NMR (CD_2Cl_2, 20 °C): δ 2.86 (m, 6H, PC*H*$(CH_3)_2$), 2.65 (m, OsCH_2; ^{1}H{^{31}P}: q, J_{HH} = 7.8 Hz), 1.34 (dvt, J_{HH} = 7.0 Hz, N = 14.0 Hz, 18H, PCH(CH_3)$_2$), 1.27 (dvt, J_{HH} = 7.0 Hz, N = 14.0 Hz, 18H, PCH(CH_3)$_2$), 1.10 (t, J_{HH} = 7.8 Hz, $OsCH_2CH_3$), −1.12 (t, J_{PH} = 24.3 Hz, 1H, Os*H*). ^{31}P{^{1}H} NMR (CD_2Cl_2, 20 °C): δ 13.3 (s).

$[Os(CH{=}CH_2)_2(NO)(P^iPr_3)_2][B(C_6H_3\text{-}3,5\text{-}(CF_3)_2)_4]$ (4). A heterogeneous mixture of $Os(H)_2Cl(NO)L_2$ (100 mg, 0.173 mmol) and $NaBAr'_4$ (161 mg, 0.182 mmol) in CH_2Cl_2 (5 mL) was freeze−pump−thaw degassed and pressurized with 1 atm of C_2H_2. After stirring the resulting deep-purple mixture at RT for 20 min, the solution was cooled to −13 °C, filtered through Celite, the solid washed with 2 × 5 mL of CH_2Cl_2, and the combined extracts concentrated to ca. 4 mL and layered with pentane (15 mL). After standing at −20 °C overnight, the purple-black crystals formed were washed with cold 4:1 pentane:CH_2Cl_2, dried in vacuo, and stored at −20 °C under Ar. Yield 213 mg (0.146 mmol, 84%). ^{1}H NMR (CD_2Cl_2, 20 °C): δ 7.72 (br, 8H, *o*-$C_6H_3(CF_3)_2$), 7.56 (s, 4H, *p*-$C_6H_3(CF_3)_2$), 9.5−4 (several broad features), 2.94 (m, 6H, PC*H*$(CH_3)_2$), 1.33 (dvt, J_{HH} = 7.2 Hz, N = 14.4 Hz, 36H, PCH(CH_3)$_2$). ^{31}P{^{1}H} NMR (CD_2Cl_2, 20 °C): δ 15.7 (s). IR (CH_2Cl_2): 1768 cm^{-1} (ν_{NO}). Anal. Found (Calcd, %) for $C_{54}H_{60}BF_{24}NOOsP_2$: C 44.42 (44.49), H 3.91 (4.15), N 1.16 (0.96). ^{1}H NMR (CD_2Cl_2, −40 °C): δ 8.21 (ddt, J_{HH} = 18.0 Hz, J_{HH} = 15.0 Hz, J_{PH} not resolved, 1H, Os(C*H*CH_2)$_a$), 7.72 (br, 8H, *o*-$C_6H_3(CF_3)_2$), 7.55 (s, 4H, *p*-$C_6H_3(CF_3)_2$), 7.14 (dtd, J_{HH} = 15.0, J_{PH} = 4.0 Hz, J_{HH} = 1.2 Hz, 1H, Os(CHCH*H*)$_a$), 6.82 (dd, J_{HH} = 11.6 Hz, J_{HH} = 5.3 Hz, 1H, Os(C*H*CH_2)$_b$), 5.56 (dtd, J_{HH} = 18.0 Hz, J_{PH} = 4.0 Hz, J_{HH} = 1.2 Hz, 1H, Os(CHCH*H*)$_a$), 5.06 (m, 1H, Os(CHCH*H*)$_b$), 3.92 (ddt, J_{HH} = 11.6 Hz, J_{HH} = 3.8 Hz, J_{PH} = 2.1 Hz, 1H, Os(CHCH*H*)$_b$), 2.89 (m, 6H, PC*H*$(CH_3)_2$), 1.27 (dvt, J_{HH} = 6.9 Hz, N = 13.8 Hz, 18H, PCH(CH_3)$_2$), 1.25 (dvt, J_{HH} = 6.9 Hz, N = 13.8 Hz, 18H, PCH(CH_3)$_2$).

Reaction of 4 with Bu_4NCl. To a solution of **4** in CD_2Cl_2 generated as described above from $Os(H)_2Cl(NO)L_2$ and $NaBAr'_4$ was added Bu_4NCl (3.3 equiv), instantly giving a light-brown solution with a purple precipitate. ^{1}H NMR spectrum recorded within several hours showed complete conversion of **4** into a predominant (>90%) product, assigned as *cis,trans*-$Os(CH{=}CH_2)_2Cl(NO)(P^iPr_3)_2$. ^{1}H NMR ($CD_2Cl_2$, 20 °C): δ 8.73 (ddt, J_{HH} = 17.9 Hz, J_{HH} = 11.1 Hz, J_{PH} = 1.3 Hz, 1H, Os(C*H*CH_2)$_a$), 7.89 (ddt, J_{HH} = 18.7, J_{HH} = 13.0 Hz, J_{PH} = 3.5 Hz, 1H, Os(C*H*CH_2)$_b$), 7.72 (br, 8H, *o*-$C_6H_3(CF_3)_2$), 7.57 (s, 4H, *p*-$C_6H_3(CF_3)_2$), 6.32 (ddt, J_{HH} = 13.1 Hz, J_{HH} = 3.1 Hz, J_{PH} = 4.1 Hz, 1H, Os(CHCH*H*)$_b$), 5.89 (ddt, J_{HH} = 19.0 Hz, J_{HH} = 3.5 Hz, J_{PH} = 3.5 Hz, 1H, Os(CHCH*H*)$_b$), 5.80 (ddt, J_{HH} = 10.9 Hz, J_{HH} = 2.0 Hz, J_{PH} = 2.0 Hz, 1H, Os(CHCH*H*)$_a$), 4.84 (ddt, J_{HH} = 18.0 Hz, J_{HH} = 2.4 Hz, J_{PH} = 1.4 Hz, 1H, Os(CHCH*H*)$_a$), 3.02 (m, 6H, PC*H*$(CH_3)_2$), 1.34 (dvt, J_{HH} = 6.8 Hz, N = 13.6 Hz, 18H, PCH(CH_3)$_2$), 1.28 (dvt, J_{HH} = 6.8 Hz, N = 13.6 Hz, 18H, PCH(CH_3)$_2$). ^{31}P{^{1}H} NMR (CD_2Cl_2, 20 °C): δ −11.5 (s).

X-ray Structure Determinations. (a) $[Os(H)_2(\eta^2\text{-}C_2H_4)(NO)(P^iPr_3)_2][PF_6]$. A crystal of suitable size was mounted using silicone grease and transferred to a goniostat where it was cooled to −160 °C for characterization and data collection. A preliminary search for peaks followed by analysis using programs DIRAX and TRACER revealed a primitive orthorhombic cell. After intensity data collection, the conditions $k + l = 2n$ for $0kl$ and $h = 2n$ for $hk0$ limited the choice of space group to $Pn2_1a$ or $Pnma$. The choice of $Pnma$ was later proven correct by the successful solution of the structure. An analytical correction was made for absorption and data processing then produced a set of 3356 unique intensities and an R_{av} = 0.041 for the averaging of 3352 of these which had been measured more than once. Four standards measured every 300 data showed no significant trends. The structure was solved using a combination of direct methods (MULTAN78) and Fourier techniques. The position of the osmium atom was obtained from an initial E-map. The remaining non-hydrogen atoms were obtained from iterations of a least-squares refinement followed by a difference Fourier calculation. One of the carbons, C(14), in one of the i-Pr groups was involved in a well resolved disorder with a position labeled C(19). These were included at 0.5 occupancy. Hydrogens bonded to carbons, including the disordered ones, were included in fixed calculated positions with thermal parameters fixed at one plus the isotropic thermal parameter of the parent carbon. In the later stages of refinement, two peaks of reasonable height were observed in chemically reasonable positions for two anticipated hydrogens bonded to osmium. An attempt to refine them was unsuccessful and eventually they were fixed at their difference Fourier positions and their thermal parameters were fixed at 4.0 which was a typical value for the other hydrogens. The cation lies in a mirror plane which contains Os(1), N(3), O(4), H(1), and H(2) and bisects the ethylene ligand. The PF_6 anion is at a center of symmetry. The largest peak in the final difference map was an osmium residual of 1.9, and the deepest hole was −2.1 e/Å^3.

(b) $[Os(CH{=}CH_2)_2(NO)(P^iPr_3)_2][B(C_6H_3\text{-}3,5\text{-}(CF_3)_2)_4]$ (4). The diffraction data were found to have monoclinic symmetry, with systematic absences characteristic of centrosymmetric space group *C*2/*c* or acentric space group *Cc*. The centrosymmetric group was chosen based on intensity statistics, and this choice was confirmed by subsequent successful structure solution and refinement. Data were corrected for Lorentz, polarization, and absorption effects, and averaged. The structure was solved by direct methods and completed by Fourier techniques. Hydrogen atoms were placed in calculated positions and refined according to a riding model during the final cycles of least squares. The borate anion is well-ordered, with the boron atom located on a crystallographic 2-fold axis. The cation, however, is disordered about a crystallographic inversion center, with the osmium atom displaced about 0.22 Å from the center. The disorder was fully resolved, but some geometric thermal parameter restraints were required for successful refinement of the near-overlapping atomic positions of the two disorder components, particularly those of the phosphine alkyl groups. The phosphine carbon atoms were refined isotropically; all other non-hydrogen atoms were refined anisotropically. No geometric restraints were applied to the C_2H_3 or NO ligands during the final cycles of refinement. The disorder undoubtedly accounts for the fairly large standard uncertainties in the interatomic distances and angles of the cation; the uncertainties in the anion's geometric parameters are much smaller. A final difference electron density map was clean, except for a single peak of 2.02 e/Å^3 residing near the osmium atom. All other difference peaks were less than 0.9 e/Å^3.

Computational Details. DFT (B3LYP)[11] calculations were carried out using Gaussian 94[12] with the standard LANL2DZ[13] basis set used with the LANL2DZ pseudopotentials for Os,[13b] P,[13c] and Cl.[13c] All structures obtained were confirmed to be real minima or transition states via frequency analysis, which was also used to calculate ZPE without scaling. For all transition states, motion corresponding to the imaginary

(11) (a) Becke, A. D. *J. Chem. Phys.* **1993**, *98*, 5648. (b) Lee, C.; Yang, W.; Parr, R. G. B. *Phys. Rev. B* **1988**, *37*, 785.

frequency was visually checked, and most structures were visually optimized to the minima they connected after correspondingly perturbing the TS geometry.

(12) Frisch, M. J.; Trucks, G. W.; Schlegel, H. B.; Gill, P. M. W.; Johnson, B. G.; Robb, M. A.; Cheeseman, J. R.; Keith, T.; Petersson, G. A.; Montgomery, J. A.; Raghavachari, K.; Al-Laham, M. A.; Zakrzewski, V. G.; Ortiz, J. V.; Foresman, J. B.; Cioslowski, J.; Stefanov, B. B.; Nanayakkara, A.; Challacombe, M.; Peng, C. Y.; Ayala, P. Y.; Chen, W.; Wong, M. W.; Andres, J. L.; Replogle, E. S.; Gomperts, R.; Martin, R. L.; Fox, D. J.; Binkley, J. S.; Defrees, D. J.; Baker, J.; Stewart, J. P.; Head-Gordon, M.; Gonzalez, C.; Pople, J. A. *Gaussian 94*, Revision D.1; Gaussian, Inc.; Pittsburgh, PA, 1995.

(13) (a) Dunning, T. H., Jr.; Hay, P. J. In *Modern Theoretical Chemistry*; Schaefer, H. F., III, Ed.; Plenum: New York, 1976; pp 1−28. (b) Hay, P. J.; Wadt, W. R. *J. Chem. Phys.* **1985**, *82*, 299. (c) Wadt, W. R.; Hay, P. J. *J. Chem. Phys.* **1985**, *82*, 284.

Acknowledgment. This work was supported by the donors of the Petroleum Research Fund, administered by the American Chemical Society.

Supporting Information Available: Full crystallographic data on $[Os(H)_2(C_2H_4)(NO)(P^iPr_3)_2][PF_6]$ and $[Os(CH{=}CH_2)_2(NO)(P^iPr_3)_2][BAr'_4]$, in CIF format. This material is available free of charge via the Internet at http://pubs.acs.org.

OM000901G